Tracing and testing the COVID-19 contact chain: cost-benefit tradeoffs

Jungyeol Kim*, Xingran Chen, Shirin Saeedi Bidokhti, & Saswati Sarkar

School of Engineering and Applied Science, University of Pennsylvania, Philadelphia, PA 19104, United States

Traditional contact tracing for COVID-19 tests the direct contacts of those who test positive even if the contacts do not show any symptom. But, why should the testing stop at direct contacts, and not test secondary, tertiary contacts or even contacts further down? The question arises because by the time an infected individual is tested the infection starting from him may have infected a chain of individuals. One deterrent in testing long chains of individuals right away may be that it substantially increases the testing load, or does it? We investigate the costs and benefits of testing the contact chain of an individual who tests positive and discover that it can both substantially reduce the cumulative infection count over time and reduce the testing load over time. We also discover a phenomenon of diminishing return beyond a threshold value on the depth of the chain to be tested in one go, the threshold then provides the most desirable tradeoff between benefit in terms of reducing the cumulative infection count and cost in terms of increasing the testing load.

To slow down the spread of COVID-19, public health authorities like the US Center for Disease Control and Prevention (CDC) have recommended to test those who have in the recent past been in physical proximity with a patient who has tested positive, even when the contacts

do not exhibit any symptom [23]. This preemptive action, commonly known as contact tracing, is deployed because given how contagious the disease is, a patient is likely to have passed on the contagion to his contacts, and the infected contacts have the potential to infect others even before they show symptoms [10]. Moreover, the CDC estimates that up to 70% percent of the infected individuals are asymptomatic, showing no symptom throughout the entire course of the disease [21], and clinical research has revealed that the asymptomatic individuals can infect others [13, 22]. Testing and isolating the infected can stop these infected individuals from spreading the disease early on, that is, while they do not show symptoms, as compared to the strategy that tests only those who show symptoms and seek medical help. Slowing down the spread by testing the contacts comes at the cost of an increase in the testing load as compared to the latter policy, yet, the cost-benefit tradeoff for contact tracing is understood to be substantially favorable (cost is the testing load, benefit is the ability to contain the outbreak).

A question that naturally arises is if cost-benefit tradeoffs may be enhanced through generalizations of the core concept of contact tracing - this is what we seek to answer in this paper. In the time that elapses between when an individual is infected and until he is tested, the disease spreads from him through a chain of several hops - he infects those he is in contact with, those he infects infect their contacts, the infected contacts infect their contacts, and so on. Fewer people are likely to be infected if we preemptively test not only the direct contacts of an individual who tests positive, but contacts of the contacts and so on. Such testing will enable us to identify and isolate the individuals further down the chain who have imbibed the disease, earlier than if we had tested only the direct contacts of those who have tested positive and reached down the chain progressively.

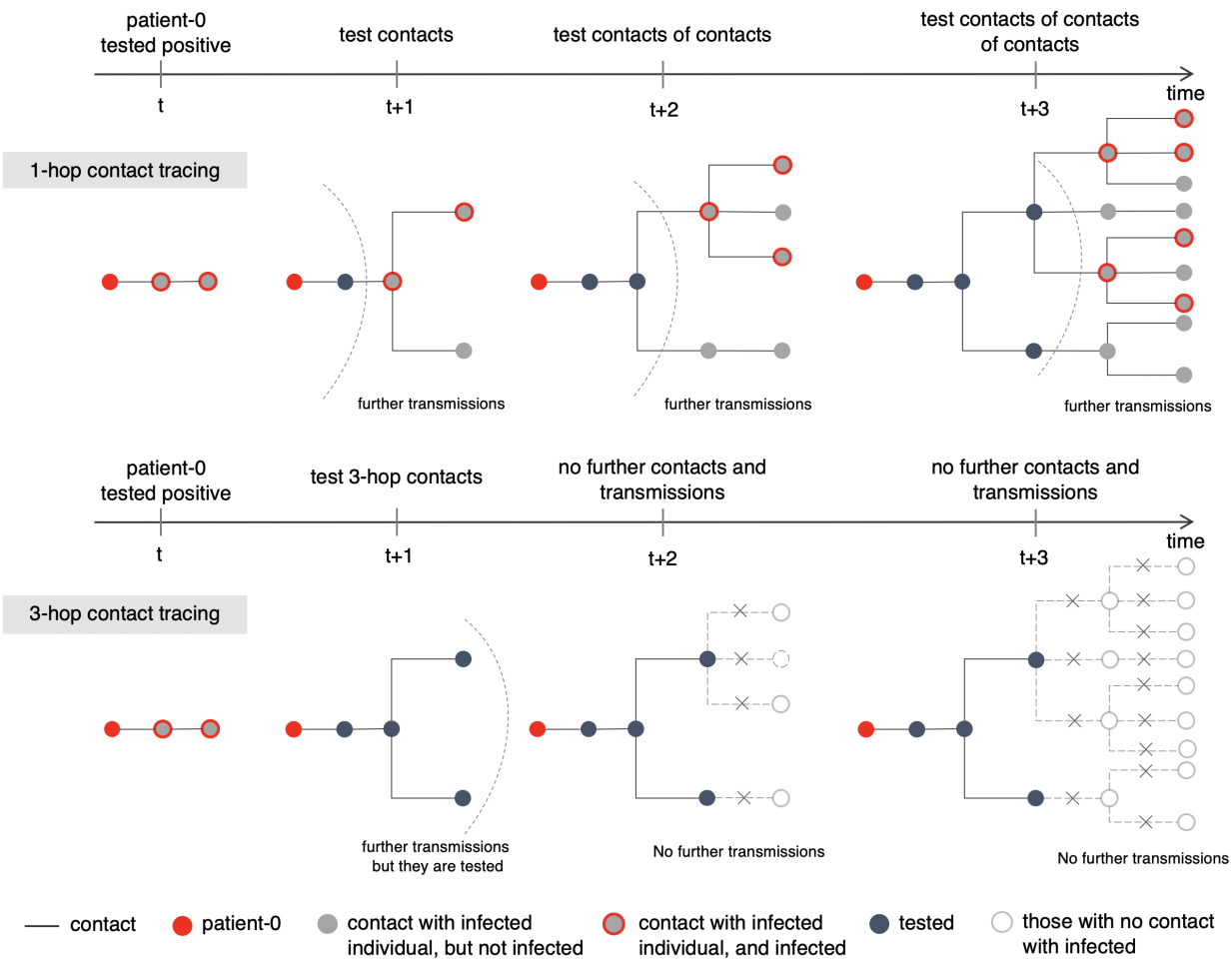

Figure 1: **Illustration of multi-hop contact tracing.** *Illustration of* 1*-hop contact tracing (i.e., testing only the direct contacts of those who test positive) and* 3*-hop contact tracing (i.e., testing the direct, secondary and tertiary contacts of those who test positive). The time at which a health authority tests the patient-*0 *(red) was after the infection has propagated* 2 *hops. By* $t+3$ *time units, both testing policies test* 4 *individuals (black) other than the patient-*0*; the* 3*-hop policy tests and isolates the positive ones in a shorter time, while* 1*-hop tests and isolates them progressively and therefore over longer times. Accordingly, only* 3 *individuals are infected under the* 3*-hop policy, while* 10 *individuals are infected under the* 1*-hop policy.*

Earlier isolation of the infected reduces the number they infect. Does such aggressive preemptive testing schemes necessarily increase the overall number of tests? The answer is not apriori clear as reduction in overall infection spread through such a testing strategy may eventually reduce the number of tests required, as illustrated in Figure 1.

We formalize this aggressive preemptive testing scheme as k-*hop contact tracing* (k), where $k = 0$ does not trace contacts and tests only those who show symptoms and seek medical help, $k = 1$ is the traditional contact tracing that tests the direct contacts of an individual who tests positive, $k = 2$ additionally tests the contacts of the contacts, $k = 3$ tests yet another hop of contacts, and so on. Our investigation will quantify the 1) benefits i.e., reduction in the number of individuals infected over time, 2) costs, i.e., increase in total number of tests, with increase in k, for a wide variety of disease parameters, contact patterns, extent of willingness of individuals to cooperate with the health officials on testing. We investigate for a wide variety of the above parameters because values of the parameters that arise in practice are not definitively known at this nascent stage of research on the novel disease, and will in general be different for different ambiences. The goal of our investigation is to reveal if this natural generalization has any merit and provide specific policy recommendations with respect to testing strategies. We will also examine whether there arises the principle of diminishing return, that is, increasing the number of hops beyond a certain *threshold* only marginally decreases the infection count but noticeably increases the testing load - if so, such threshold, which we seek to identify, provides the optimum cost-benefit tradeoff.

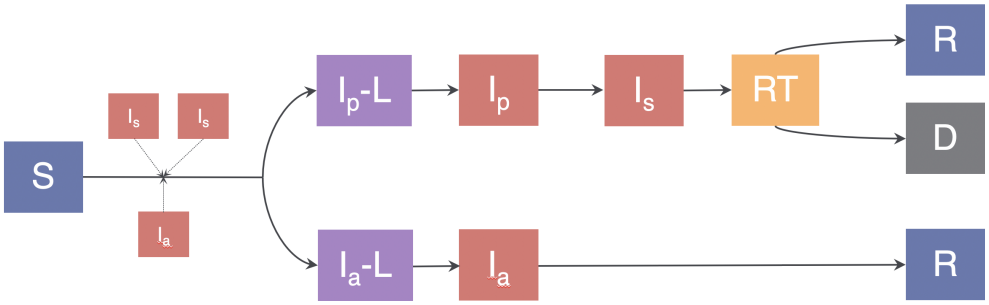

Figure 2: **Virus transmission model illustration.** *The Compartmental model consists of the following compartments: Susceptible (S), Presymptomatic-Latent (I_p-L), Presymptomatic (I_p), Symptomatic (I_s), Ready-to-Test (RT), Asymptomatic-Latent (I_a-L), Asymptomatic (I_a), Recovered (R), and Dead (D).*

The significance of our investigation also draws from the fact that the testing recommendations by the regulating authorities have not been finalized yet, and recommendations are being continually adapted as new facets are being discovered. For example, in the last few months the CDC has changed its recommendation about testing the asymptomatic individuals multiple times [22].

We consider a discrete time stochastic evolution of COVID-19 in a population that initially consists of susceptible and a few contagious individuals. We model the progression of the disease using a compartmental model (Figure 2). The disease spreads from the contagious to the susceptible individuals through mutual interaction. In any given interaction with a contagious individual, a susceptible is infected with a probability. After a *latency period* (the presymptomatic-latent and asymptomatic-latent are in this latency period), the newly infected individuals become contagious. Specifically, at the end of the latency period, the individuals either become *presymptomatic*

(the stage before exhibiting symptoms), or *asymptomatic* (that is, they never show symptoms). Presymptomatics proceed to become *symptomatics* in the next stage. Presymptomatics, asymptomatics, symptomatics all however are contagious.

We assume that test results are obtained in the same day, owing to the availability of reliable RT-PCR and antigen tests that are able to do so [9, 19] (recent antigen test authorized by the FDA under an emergency use can give results in 15 minutes with 97.1% sensitivity).

We consider cases in which only a fraction of contacts can be tested, as they either do not consent or can not be traced; we refer to this fraction as *cooperativity*. We assume that the contacts who can be identified are identified within a day, such turnaround times are for example attainable if individuals install contact tracing apps [7] in their wearable or hand-held devices which continually and automatically record all contacts and communicate to the authorities once an individual tests positive or is alerted of direct or indirect exposure. Tests can then be scheduled the next day through the same apps.

The probability with which an infected individual infects a susceptible in an interaction depends on various factors such as the duration, environment (e.g., indoor or outdoor) of the interaction, protective gears worn by the individuals involved etc. Since different environments and behavioral patterns have different values of this probability, we consider a range of values, namely, $0.04, 0.2, 0.4$ respectively, for symptomatic individuals. We consider that a presymptomatic individual infects a susceptible individual with the same probability as a symptomatic individual, and refer to this probability as the *probability of infection*. We consider that an asymptomatic individual

infects a susceptible with 0.75 times this probability [21].

We have simulated k-hop contact tracing for $k = 0, 1, 2, 3$ to large values of k for 1) a data-driven time-varying network, obtained from data individuals in Tokyo, Japan provide over a social network about their locations and the corresponding time-stamps [25] and 2) various static synthetic topologies (of Erdős Rényi random network and scale-free networks) in which connections do not change with time. We choose these two broad categories to complement each other and represent various human contact patterns. The first captures a certain semblance of reality in that it is obtained from spatial and temporal records of actual human presence over a time period; here the contact patterns vary over time which is also what happens in reality. Yet, it is constructed from only one set of data, which may not be representative of all contact patterns. We therefore examine whether the phenomena observed in it also recurs in some other very different networks, namely in two examples of classical synthetic networks: Erdős Rényi and scale-free networks. These examples complement each other in some fundamental characteristics such as in the nature of the degree distribution. The degrees of the nodes represents the number of contacts of the corresponding individuals. The Erdős Rényi network is more regular, in that there is relatively low variance in the degree distribution. The scale-free network, on the other hand, has some nodes with high degrees (perhaps representing celebrities who interact with a large number of individuals) and many more nodes with low degrees (representing common folks); the degree distribution therefore has a high variance. Any phenomenon that is observed in the three very different types of networks modeling human contact patterns (the data-driven time-varying network and the two static synthetic networks) is likely to recur extensively.

Refer to Methods for details on the systems we consider, the parameters we choose and further justification for the choices and the limitations thereof.

Results

We start with a summary of our important findings from the simulations for k-hop contact tracing that we perform for $k = 0, 1, 2, 3, \ldots$. We observe the following for *multi-hop* testing, which is k-hop contact testing for $k > 1$:

- *Benefit of multi-hop contact tracing:* Multi-hop contact tracing considerably reduces the total number of infections over time compared to 1-hop contact tracing (that is, the traditional contact tracing). The reduction is higher with 1) increase in probability of infection 2) the decrease in cooperativity 3) decrease in the latency period. In addition, multi-hop contact tracing substantially reduces the average daily new infection count in the *peak infection period* (time until the daily new infection count peaks) compared to 1-hop contact tracing.

- *Cost of multi-hop contact tracing:* Over time the overall number of tests required in multi-hop contact tracing is usually *lower*, than that in 1-hop contact tracing. But, studying how the number of tests changes with time, initially the number of tests needed for multi-hop is somewhat (considerably in few instances) higher than for 1-hop contact tracing.

Increasing the value of k from $k = 1$, the number of infections and the number of tests over time decreases up to a threshold value of k (we observe that this threshold value is $k = 2$ or $k = 3$

in our simulations). Formally, we define the threshold point as the value of k at which the overall number of tests required (cost) is minimized. As k increases beyond this threshold value, we see a phenomenon of *diminishing return*, that is, the number of infections only marginally decreases and number of tests increases (considerably, in some instances).

We substantiate the above findings with the results reported in Figures 3 and 5, Figure 3 for data-driven time-varying network and Figure 5 for static synthetic topologies. In each case we report the average of 1000 simulation runs on given topologies.

We first consider the highest probability of infection (i.e., 0.4) and lowest cooperativity (i.e., 0.2) from our range of choices. As k increases from 0 to 3, the cumulative number of infections considerably decreases, and subsequently decreases only marginally with further increase in k. 3-hop contact tracing achieves 81% reduction in the cumulative number of infections compared to no-contact tracing, while 1-hop contact tracing achieves only 24% reduction (first column in Figure 3a). The total number of tests for k-hop contact tracing steadily decreases with increase in k from $k = 1$ to $k = 3$, and subsequently steadily increases as k increases further. This number is minimized for 3-hop contact tracing, at which value 37% fewer tests are required, overall, than 1-hop tracing (first column in Figure 3a). Thus, the threshold value is $k = 3$. The daily number of tests is somewhat higher initially for multi-hop contact tracing, but rapidly declines soon, as compared to 1-hop contact tracing (Figure 4), leading to overall fewer number of tests for multi-hop contact tracing. These observations may be explained as follows. Multi-hop contact tracing may test greater number of individuals in early stages because it traces up to more hops even

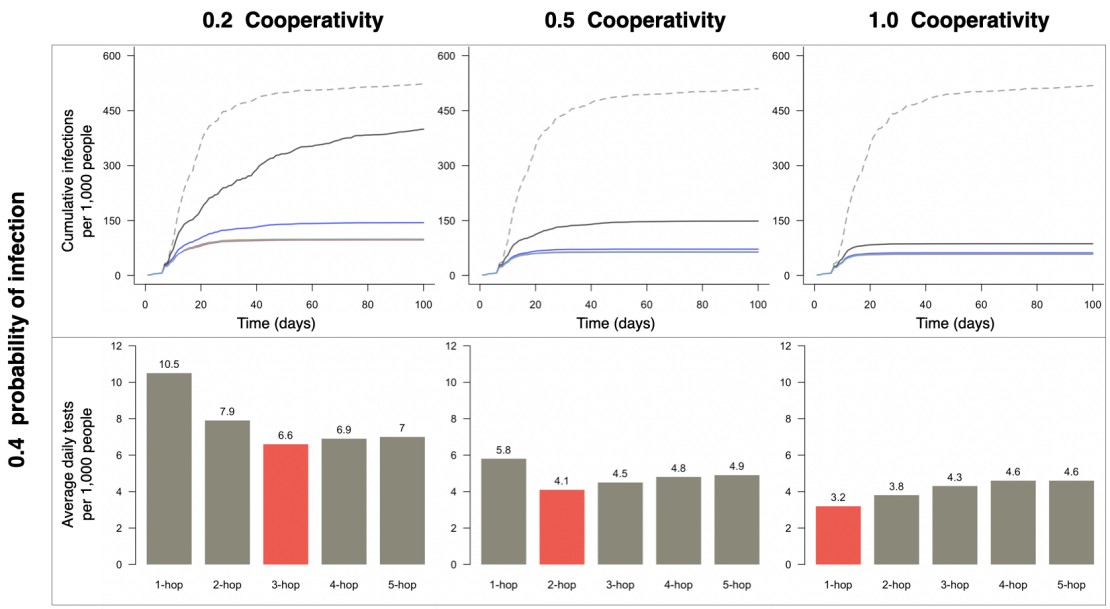

(a)

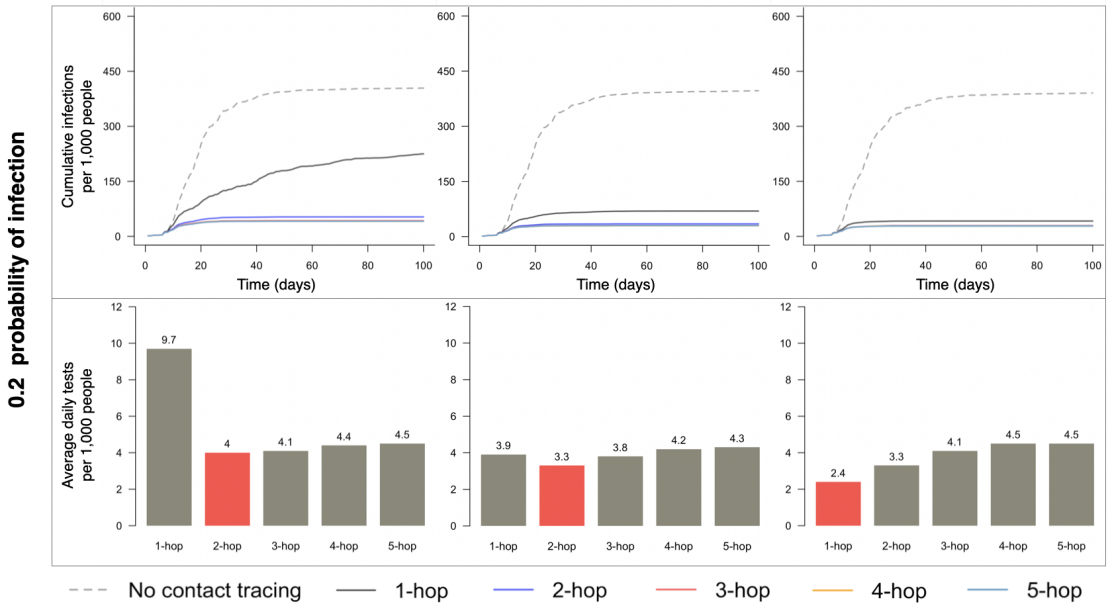

(b)

Figure 3: **The cumulative number of infections and average daily tests required for k-hop contact tracing for various values of k for data-driven time-varying network.** *The red colored bar corresponds to the threshold value of k. For k exceeding the threshold value, the curves for the cumulative number of infections heavily overlap and become indistinguishable.*

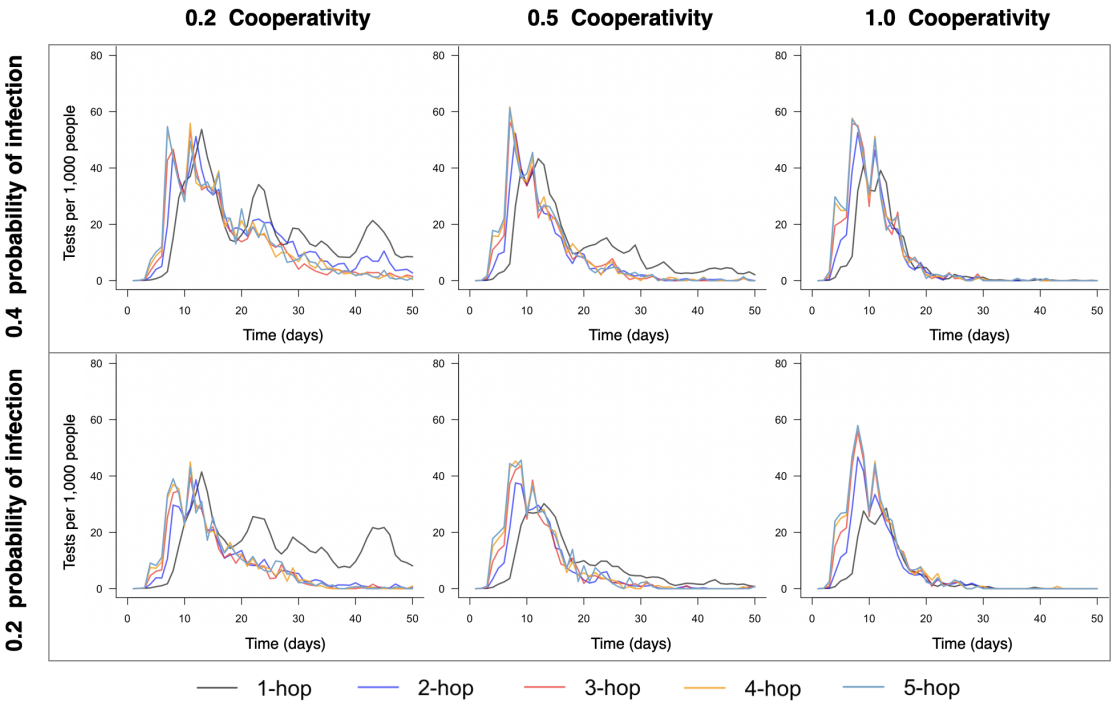

Figure 4: **The number of tests over time for data-driven time-varying network.**

from the same number of confirmed cases. However, this aggressive preemptive testing from early stages can rapidly mitigate the spread of infection earlier than 1-hop contact tracing through early identification and quarantining of the infected, thus fewer number of individuals transmit the virus and need tests with passage of time. The latter phenomenon more than compensates for the larger number of tests required in early stage for multi-hop contacts of those who test positive.

All the phenomena reported above is replicated for other parameters for data-driven time-varying networks (other subfigures of Figure 3), but the extent of the advantage and values of the thresholds differ. We comment on the insights the differences provide.

When cooperativity increases to 1, the efficacy of 1-hop tracing increases substantially, it

reduces cumulative infections by 83% compared to 0-hop tracing (third column in Figure 3a). Comparing the results for cooperativities of 1 and lower, we note that multi-hop contact tracing can offset the limitation arising from the lack of available information on contacts.

As probability of infection decreases, 1-hop contact tracing becomes more and more effective, and the threshold value generally decreases (or remains the same). Refer to Figure 3b for the intermediate value of 0.2 for the probability of infection, and to Figure 7 in Supplementary Information for the lowest value of 0.04.

We consider static synthetic networks now (Figure 5). All the phenomena reported above is replicated, but the specifics differ. When probability of infection is 0.4, the threshold value is 2 for both the scale-free and Erdős Rényi networks (first column in Figure 5). In the two cases, despite the fact that the overall number of tests required in 2-hop contact tracing is significantly lower than that in 1-hop contact tracing, 2-hop contact tracing reduces the cumulative number of infections by 96% and 98%, respectively compared to 0-hop tracing, while 1-hop tracing reduces by 56% and 41%, respectively. The phenomenon of diminishing return is even more accentuated in these as the number of tests sharply increase with increase in k beyond $k = 2$ for $k-$hop contact tracing. Also, considering the variation of the number of tests over time, we notice that in scale-free networks, the number is significantly higher for multi-hop contact tracing than that for 1- hop contact tracing *initially* (Figure 6). But, the decline in the number of tests required for multi-hop contact tracing becomes equally precipitous over time, and the rapid decline starts in a short time from the start of the testing period as well. Figure 5 plots the average of 1000 simulation runs over 1 realization of

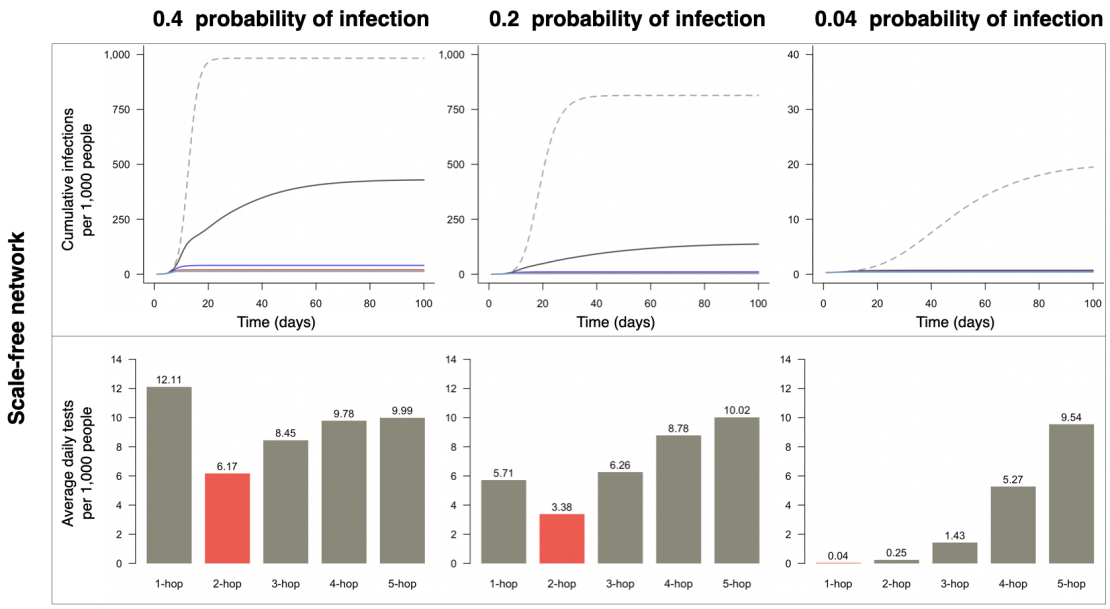

(a)

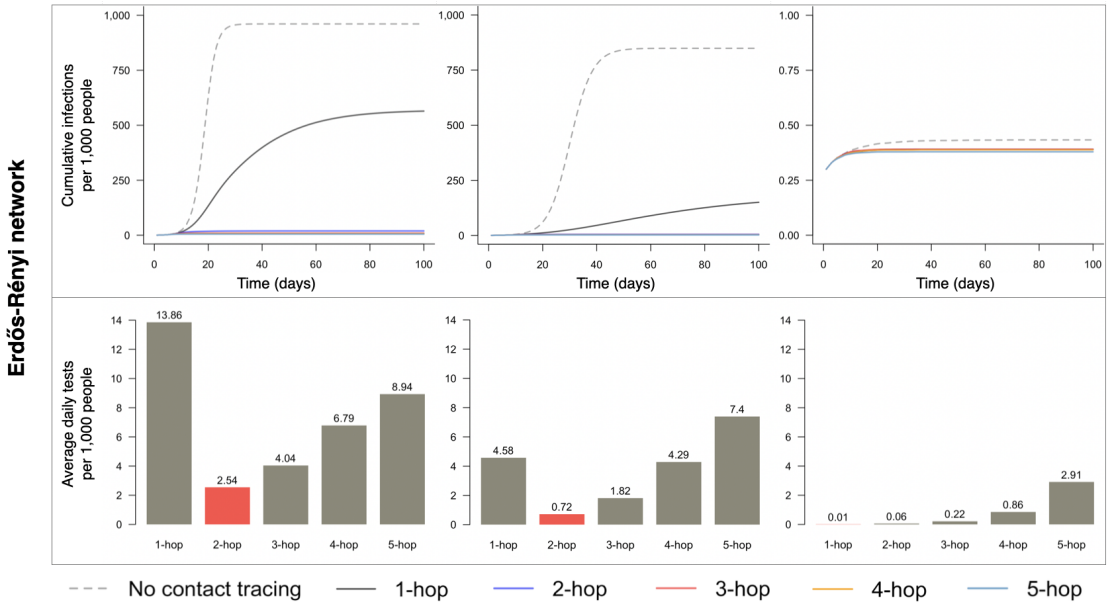

(b)

Figure 5: **The cumulative number of infections and average daily tests required for k-hop contact tracing for various values of k for static synthetic networks.** *The red colored bar corresponds to the threshold value of k. For k exceeding the threshold value, the curves for the cumulative number of infections heavily overlap and become indistinguishable.*

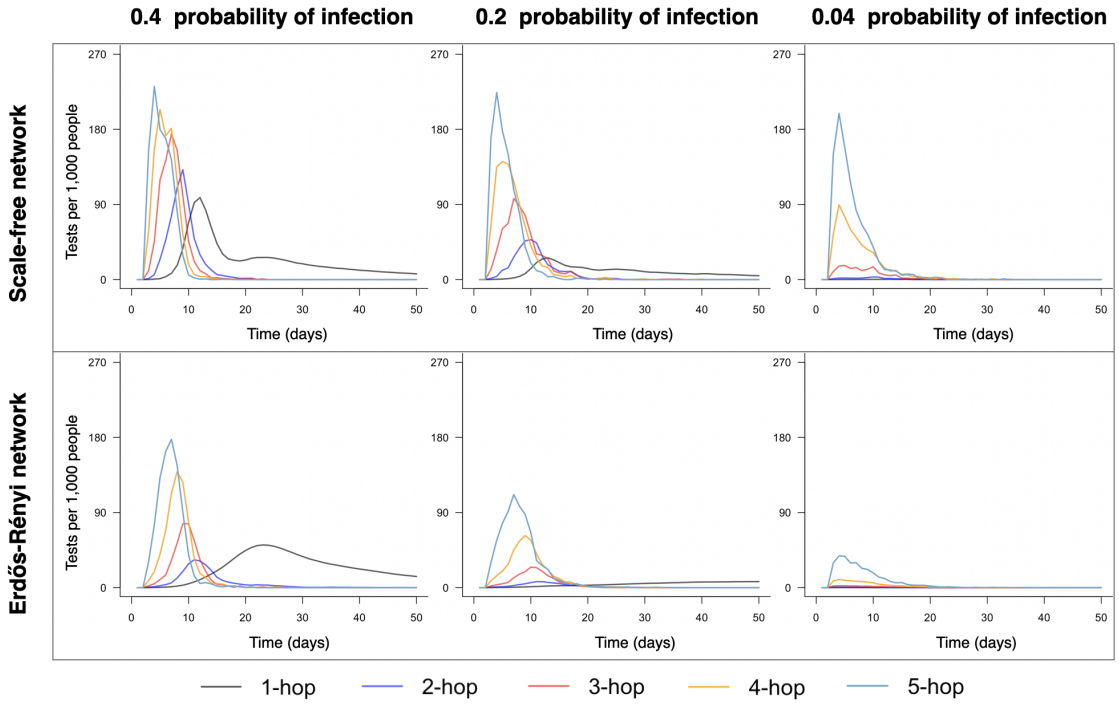

Figure 6: **The number of tests over time for static synthetic networks.**

the static synthetic topologies, Figure 9 in Supplementary Information reports the average of 100 runs over 10 realizations of the same static synthetic topologies, corresponding plots in Figure 5 and Figure 9 show identical trend.

We now focus on the peak infection period and the average daily new infection count during this period. The duration of this period is a measure of how soon the infection is contained. The average daily new infection count during this period is a measure of the treatment-load health care centers experience in a critical period in which these have the potential to be overwhelmed. Under multi-hop contact tracing the peak infection period is shorter, in some cases considerably shorter, and the average daily new infection count during this period is invariably substantially lower, and therefore the healthcare facilities run lower risk of being overwhelmed. For example,

in the data-driven time-varying network, considering the parameters as the first column in Figure 3a, for 3-hop contact tracing, the peak infection period is 7 days and an average of 3.6 (per 1000 population) daily new infections occurs during this period. On the other hand, for 1-hop contact tracing, the peak infection period is 11 days, and an average of 8.6 (per 1000 population) daily new infections occurs during this period. Next, in scale-free and Erdős Rényi networks, considering the parameters as the first column in Figure 5, under 2-hop contact tracing, the peak infection periods are 8 and 10 days, respectively, and an average of 3 (per 1000) and 1.1 (per 1000) daily new infection occurs during this period, respectively. On the other hand, for 1-hop contact tracing in these topologies, the peak infection periods are 10 and 22 days, respectively, and an average of 8.9 (per 1000) and 7.7 (per 1000) daily new infections occurs during this period, respectively. Note that multi-hop contact tracing substantially reduces the peak infection period in scale-free networks.

We now examine how increase in the latency period affects the results. In this case, the infected individuals become contagious later, thus, the potential of 1-hop contact tracing to detect and remove individuals before they become contagious or in the early period of their becoming contagious increases. Comparing the results for randomized latency periods of two different means, we note that this is indeed the case. In data-driven time-varying network, when the mean latency period is 1 day (2 days, respectively), 1-hop contact tracing can achieve 24% (33%, respectively) reduction in the cumulative number of infections compared to 0-hop contact tracing, and 3-hop contact tracing can achieve 81% (86%, respectively) reduction. In scale-free network, when the mean latency period is 1 day (2 days, respectively), 1-hop contact tracing can achieve 56% (71%,

respectively) reduction in the cumulative number of infections compared to 0-hop contact tracing, and 2-hop contact tracing can achieve 96% (98%, respectively) reduction. In Erdős Rényi network, when the mean latency period is 1 day (2 days, respectively), 1-hop contact tracing can achieve 41% (58%, respectively) reduction in the cumulative number of infections compared to 0-hop contact tracing, and 2-hop contact tracing can achieve 98% (99%, respectively) reduction. Refer to Figure 10 in Supplementary Information for a bar-graph representation of this data.

Discussion

Our findings obtained through extensive simulations over a diverse set of contact topologies, starting from data-driven time-varying networks to static synthetic networks show that multi-hop testing has the potential to substantially reduce total number of infections (which would in turn reduce fatalities and treatment load on healthcare facilities) and reduce overall testing load. It also helps contain COVID-19 outbreaks within shorter times and reduces average daily new infection counts, specifically in the period up to when the daily new infection count peaks, which would in turn reduce the treatment load on healthcare facilities during the peak period. All these collectively have the potential to contain the outbreak without extensive lockdowns and economic downturns.

Our findings lead to the following recommendations for public health authorities:

- Deploy multi-hop testing; usually testing up to secondary or tertiary contacts of those who test positive suffices.

- The recommended number of hops are on the higher end of the above range when: 1) the probability of infection in each contact is high (e.g., from indoor contacts, longer durations of contacts, lack of protective gears) 2) cooperativity is low 3) the latency period is short.

- Create the infrastructure for handling a larger testing load for limited periods, which will lead to a reduction in the overall testing load over time with the daily testing load expected to decline shortly after the testing starts (if multi-hop testing is deployed).

Finally, multi-hop testing may provide similar benefits for other infectious diseases which exhibit silent propagation (infection from individuals who do not show symptoms).

Note that the contact tracing recommendation of the CDC involves both testing and quarantining (even when the test result is negative) the direct or primary contacts of those who test positive. Along the same lines, recent works considered tracing and quarantining the direct contacts of those who tested positive [1, 7, 11]. Another recent work considered tracing and quarantining both primary and secondary contacts of those who test positive, and found that quarantining secondary contacts decreases the cumulative infection count compared to quarantining only the primary contacts, but also requires substantially higher number of quarantines [8]; this work appears to reject the notion of quarantining secondary contacts and did not therefore explore quarantining tertiary or even more distant contacts. It does not investigate testing the primary and secondary contacts, perhaps because they would be quarantined regardless of the test results. We instead explore tracing and testing multi-hop contacts, testing eliminates the need for extensive quarantining as only those who test positive need to be quarantined. Our results show that multi-hop testing even re-

duces the number of tests required. The difference between our finding and the recent work arises because quarantine is a cumulative process in which each contact is quarantined for several days, while tests related to each positive patient are done only once. As to the primary contacts of those who test positive, we take no position on whether they should be quarantined even when they test negative, and leave that to the policies of the relevant public health authorities.

We now discuss the scenarios in which some of our assumptions may not hold. Tracing contacts and scheduling tests for those traced may require more than a day when individuals do not use contact tracing apps. PCR test results are not obtained same day if the testing site and laboratory are not co-located, though this delay may not affect the broad nature of our findings if those tested quarantine until the test results are known. Antigen tests give results in an hour but some of them reportedly record non-negligible proportion of false negatives. Depending on classifiers such as duration, environment (indoor or outdoor), usage of protective gears, different contacts may pass on infection with different probabilities. Assuming that such a probability is identical for all contacts with same infectious categories, which is what we did, is equivalent to considering an average over all contacts. Explicitly investigating the impact of 1) delay in tracing contacts and obtaining test results 2) errors in test results 3) non-uniform infection probabilities constitute directions for future research.

Methods

Construction of data-driven time-varying network. Our goal has been to evaluate the multi-hop contact tracing strategy using publicly-available data of human contact patterns. For evaluating the

impact of multi-hop contact tracing, data sets need to involve large population sizes, otherwise length of the contact chains will be limited by the size of the target populace. Also, in reality, pandemic spread involves large target populaces. Data of human contact patterns is not plentiful in the public domain due to privacy and other concerns, the availability becomes even less for contact patterns of large population sizes. We utilized the data that users of Foursquare service (a Location-Based Social Networking or LBSN) made available in Social Media about their locations in Tokyo, Japan along with time-stamps. This dataset contains advertised locations (or check-ins) collected for about 10 months (from 12 April 2012 to 16 February 2013). Each check-in contains information about the time at which the user visited the location, the GPS coordinates of the locations, and the nature of the locations (e.g., coffee shops, restaurants etc.) [25]. We use the first 100 days of data with at least one check-in. The strength of this data set is that it provides actual time-stamped locations of a large number of individuals, more than 2000, over a long period of time. The weakness is that the contacts are still sparser than what arises in reality as the locations in question are usually crowded and much larger number of individuals actually visit these locations in overlapping time intervals but their whereabouts are not being reported in this dataset as they do not use this LBSN. The contact network will become denser if their presence can be considered. To compensate for this artificial sparsity we construct contact patterns based on the available data by postulating that people have had a contact if they have been at the same venue in the same day. During such a contact a contagious individual passes the disease on to a susceptible individual with a certain probability (we mention how we choose these probabilities where we provide details on the Compartmental model of virus transmission and in Table 1 in Supplementary Information).

Note that in reality individuals who have been at the same location in the same day do not always do so at the same time and are therefore not always in physical proximity to pass on the disease from one to another. Thus, the contact pattern we consider is denser than what the dataset actually provides, which may compensate for the artificial sparsity in question. The constructed data-driven time-varying contact patterns has 5553.71 daily interaction on average among 2120 individuals. The evaluations can be repeated on more accurate and expansive contact patterns as they become available through collective efforts and enrichment of existing data repositories.

Static synthetic networks The static topologies consist of scale-free network [2, 3] and Erdős Rényi random network [3, 6]. Figure 5 have been provided for only one realization of scale-free network and Erdős Rényi random network, Figure 9 in Supplementary Information however shows plots of averages over 10 realizations of each.

The scale-free network topologies are generated by Barabási-Albert method where new nodes are added at each time step with 2 links that connect to existing nodes with a probability being proportional to the degree of the existing nodes. We consider topologies of $10,000$ nodes and $19,997$ edges, thus average degree of a node is $\langle k \rangle = 3.9994$. For the single realization we use in Figure 5a, diameter and average path length are 9 and 5.01, respectively. Figure 8a in Supplementary Information shows that for the one realization we consider in Figure 5a, the degree distribution is well approximated by power-law with degree exponent 3, as should be for scale-free networks. Thus, the single realization in question is a typical scale-free network.

The Erdős Rényi network consists of $10,000$ nodes which are connected with $20,000$ ran-

domly placed edges, thus the average degree of a node is $\langle k \rangle = 4$. For the one realization we consider in Figure 5b, diameter (i.e., the greatest distance between pair of nodes of connected components) is 14 and average path length (i.e., average distance along the existing paths) is 6.76. Figure 8b in Supplementary Information shows that for the one realization we consider in Figure 5b, the degree distribution is well approximated by Poisson distribution with parameter $\langle k \rangle$, as should be for Erdős Rényi random networks. Thus, the single realization in question is a typical Erdős Rényi random network.

Compartmental model of virus transmission. We use a *discrete time compartmental disease model* to model the progression of COVID-19 where the transition from each compartment to the next happens after a random amount of time with a geometric distribution. Compartmental model is also used in [1, 24]. Different stages of the disease are shown in Figure 2. The Compartmental model consists of the following stages: *Susceptible (S), Presymptomatic-Latent (I_p-L), Presymptomatic (I_p), Symptomatic (I_s), Ready-to-Test (RT), Asymptomatic-Latent (I_a-L), Asymptomatic (I_a), Recovered (R)*, and *Dead (D)*. Only symptomatic individuals show symptoms, while presymptomatic, symptomatic and asymptomatic individuals infect others.

When a susceptible (S) individual comes into contact with a symptomatic (I_s) individual, he is infected with the probability of infection β_s. Similarly, a presymptomatic (I_p) and an asymptomatic (I_a) individual infects a susceptible upon contact with probabilities, $\beta_p (= \gamma_p \beta_s)$, $\beta_a (= \gamma_a \beta_s)$, respectively, where γ_p and γ_a are respectively infectiousness of presymptomatic and asymptomatic individuals relative to symptomatic individuals. If a susceptible individual i interacts with l symptomatic, m presymptomatic, and n asymptomatic individuals at time $t-1$, the

probability that the susceptible individual is infected at time t is $1-(1-\beta_s)^l(1-\beta_p)^m(1-\beta_a)^n$.

Once an individual is infected he becomes contagious after a geometrically distributed latency time, whose statistics depends on whether he will develop symptoms at some point or otherwise. Following the nomenclature in compartmental models already utilized for COVID-19, we assume that an infected individual becomes asymptomatic-latent (with probability p_a) or presymptomatic-latent (with probability $1-p_a$). The asymptomatic-latent (I_a-L) individuals never develop symptoms, do not infect others for an mean latency duration of $1/\lambda$, and subsequently become contagious, at which stage we call them asymptomatic or I_a for simplicity. An asymptomatic individual remains contagious for a geometrically distributed random duration with mean $1/r_a$, after which he recovers. We now consider the other compartment an individual enters after infection, the presymptomatic-latent compartment. A presymptomatic-latent individual becomes contagious after a mean latency period of $1/\lambda$, at which point we call him presymptomatic or I_p. He remains presymptomatic for a geometrically distributed duration with mean $1/\alpha$; after this duration he develops symptoms and is called symptomatic. A symptomatic individual continues to infect his contacts until he opts for testing (RT). The duration for which a symptomatic individual infects others is geometrically distributed with mean $1/w$. Once this duration ends, the patient quarantines himself and does not infect others. He ultimately dies (D) with probability p_d, or recovers (R) with probability $1-p_d$, after a geometrically distributed duration whose mean is $1/r_s$. We do not consider that individuals can be reinfected.

We consider that initially all but three individuals are susceptible, among the three there is one each of presymptomatic, symptomatic and asymptomatic. The parameters we choose and

further justification for the choices are listed in Table 1 in Supplementary Information.

Multi-hop contact tracing process. Every day individuals who are *ready to test* by virtue of showing symptoms are tested and isolated if they test positive. Considering an individual who tests positive on day t, we describe the process of tracing his k-hop contacts on day t and testing them on day $t+1$. On day t after the individual in question tests positive, the public health authority traces his k-hop contacts, over the last 14 days, and informs them that they may have been exposed. If cooperativity is q, only q proportion of interactions per day can be identified. Tests are scheduled on day $t+1$. Those scheduled to be tested are isolated from everyone else on the day of the test. The test results are available in the same day, and those who test positive are isolated until they recover and those who test negative can resume their normal activities. Individuals who test positive will not be tested again, but those who test negative can be tested again after 3 days from the test date if they have direct or indirect interactions with any one who tests positive or if they show symptoms.

Competing Interests The authors declare no competing interests.

Correspondence Correspondence and requests for materials should be addressed to J.K.

1. A. Aleta, D. Martín-Corral, A. P. y Piontti, M. Ajelli, M. Litvinova, M. Chinazzi, N. E. Dean, M. E. Halloran, I. M. Longini Jr, S. Merler, et al. Modelling the impact of testing, contact tracing and household quarantine on second waves of COVID-19. *Nature Human Behaviour*, 4(9):964–971, 2020.

2. A.-L. Barabási and R. Albert. Emergence of scaling in random networks. *Science*, 286(5439): 509–512, 1999.

3. A.-L. Barabási et al. *Network science*. Cambridge university press, 2016.

4. M. Biggerstaff, M. A. Jhung, C. Reed, A. M. Fry, L. Balluz, and L. Finelli. Influenza-like illness, the time to seek healthcare, and influenza antiviral receipt during the 2010–2011 influenza season—United States. *The Journal of infectious diseases*, 210(4):535–544, 2014.

5. A. W. Byrne, D. McEvoy, A. B. Collins, K. Hunt, M. Casey, A. Barber, F. Butler, J. Griffin, E. A. Lane, C. McAloon, K. O'Brien, P. Wall, K. A. Walsh, and S. J. More. Inferred duration of infectious period of SARS-CoV-2: rapid scoping review and analysis of available evidence for asymptomatic and symptomatic COVID-19 cases. *BMJ Open*, 10(8), 2020. ISSN 2044-6055. doi: 10.1136/bmjopen-2020-039856. URL `https://bmjopen.bmj.com/content/10/8/e039856`.

6. P. Erdős and A. Rényi. On the evolution of random graphs. *Publ. Math. Inst. Hung. Acad. Sci*, 5(1):17–60, 1960.

7. L. Ferretti, C. Wymant, M. Kendall, L. Zhao, A. Nurtay, L. Abeler-Dörner, M. Parker, D. Bonsall, and C. Fraser. Quantifying SARS-CoV-2 transmission suggests epidemic control with digital contact tracing. *Science*, 368(6491), 2020.

8. J. A. Firth, J. Hellewell, P. Klepac, S. Kissler, A. J. Kucharski, and L. G. Spurgin. Using a real-world network to model localized COVID-19 control strategies. *Nature Medicine*, pages 1–7, 2020.

9. G. Guglielmi. The explosion of new coronavirus tests that could help to end the pandemic. *Nature*, 2020. https://www.nature.com/articles/d41586-020-02140-8.

10. X. He, E. H. Lau, P. Wu, X. Deng, J. Wang, X. Hao, Y. C. Lau, J. Y. Wong, Y. Guan, X. Tan, et al. Temporal dynamics in viral shedding and transmissibility of COVID-19. *Nature medicine*, 26(5):672–675, 2020.

11. J. Hellewell, S. Abbott, A. Gimma, N. I. Bosse, C. I. Jarvis, T. W. Russell, J. D. Munday, A. J. Kucharski, W. J. Edmunds, F. Sun, et al. Feasibility of controlling COVID-19 outbreaks by isolation of cases and contacts. *The Lancet Global Health*, 2020.

12. S. A. Lauer, K. H. Grantz, Q. Bi, F. K. Jones, Q. Zheng, H. R. Meredith, A. S. Azman, N. G. Reich, and J. Lessler. The incubation period of coronavirus disease 2019 (covid-19) from publicly reported confirmed cases: estimation and application. *Annals of internal medicine*, 172(9):577–582, 2020.

13. S. Lee, T. Kim, E. Lee, C. Lee, H. Kim, H. Rhee, S. Y. Park, H.-J. Son, S. Yu, J. W. Park, et al. Clinical course and molecular viral shedding among asymptomatic and symptomatic patients with SARS-CoV-2 infection in a community treatment center in the republic of korea. *JAMA Internal Medicine*, 2020.

14. N. M. Linton, T. Kobayashi, Y. Yang, K. Hayashi, A. R. Akhmetzhanov, S.-m. Jung, B. Yuan, R. Kinoshita, and H. Nishiura. Incubation period and other epidemiological characteristics of 2019 novel coronavirus infections with right truncation: a statistical analysis of publicly available case data. *Journal of clinical medicine*, 9(2):538, 2020.

15. Y. Liu, L.-M. Yan, L. Wan, T.-X. Xiang, A. Le, J.-M. Liu, M. Peiris, L. L. Poon, and W. Zhang. Viral dynamics in mild and severe cases of covid-19. *The Lancet Infectious Diseases*, 2020.

16. S. Ma, J. Zhang, M. Zeng, Q. Yun, W. Guo, Y. Zheng, S. Zhao, M. H. Wang, and Z. Yang. Epidemiological parameters of coronavirus disease 2019: a pooled analysis of publicly reported individual data of 1155 cases from seven countries. *Medrxiv*, 2020.

17. J. Y. Noh, J. G. Yoon, H. Seong, W. S. Choi, J. W. Sohn, H. J. Cheong, W. J. Kim, and J. Y. Song. Asymptomatic infection and atypical manifestations of covid-19: comparison of viral shedding duration. *The Journal of Infection*, 2020.

18. D. P. Oran and E. J. Topol. Prevalence of asymptomatic SARS-CoV-2 infection: A narrative review. *Annals of Internal Medicine*, 2020.

19. R. Service. In 'milestone,' fda oks simple, accurate coronavirus test that could cost just $5. *Science*, 2020. `https://www.sciencemag.org/news/2020/08/milestone-fda-oks-simple-accurate-coronavirus-test-could-cost-just-5`.

20. The U.S. Centers for Disease Control and Prevention (CDC). COVID-19 pandemic planning scenarios. May 2020. `https://www.cdc.gov/coronavirus/2019-ncov/hcp/planning-scenarios-archive/planning-scenarios-2020-05-20.pdf`.

21. The U.S. Centers for Disease Control and Prevention (CDC). COVID-19 pandemic planning scenarios. Aug. 2020. `https://www.cdc.gov/coronavirus/2019-ncov/hcp/planning-scenarios.html#definitions`.

22. The U.S. Centers for Disease Control and Prevention (CDC). Overview of testing for SARS-CoV-2 (COVID-19). Sept. 2020. https://www.cdc.gov/coronavirus/2019-ncov/hcp/testing-overview.html.

23. The U.S. Centers for Disease Control and Prevention (CDC). Contact tracing for COVID-19. Sept. 2020. https://www.cdc.gov/coronavirus/2019-ncov/php/contact-tracing/contact-tracing-plan/contact-tracing.html.

24. C. J. Worby and H.-H. Chang. Face mask use in the general population and optimal resource allocation during the COVID-19 pandemic. *medRxiv*, 2020.

25. D. Yang, D. Zhang, V. W. Zheng, and Z. Yu. Modeling user activity preference by leveraging user spatial temporal characteristics in LBSNs. *IEEE Transactions on Systems, Man, and Cybernetics: Systems*, 45(1):129–142, 2014.

26. R. Zhou, F. Li, F. Chen, H. Liu, J. Zheng, C. Lei, and X. Wu. Viral dynamics in asymptomatic patients with covid-19. *International Journal of Infectious Diseases*, 2020.

27. L. Zou, F. Ruan, M. Huang, L. Liang, H. Huang, Z. Hong, J. Yu, M. Kang, Y. Song, J. Xia, et al. SARS-CoV-2 viral load in upper respiratory specimens of infected patients. *New England Journal of Medicine*, 382(12):1177–1179, 2020.

Supplementary Information

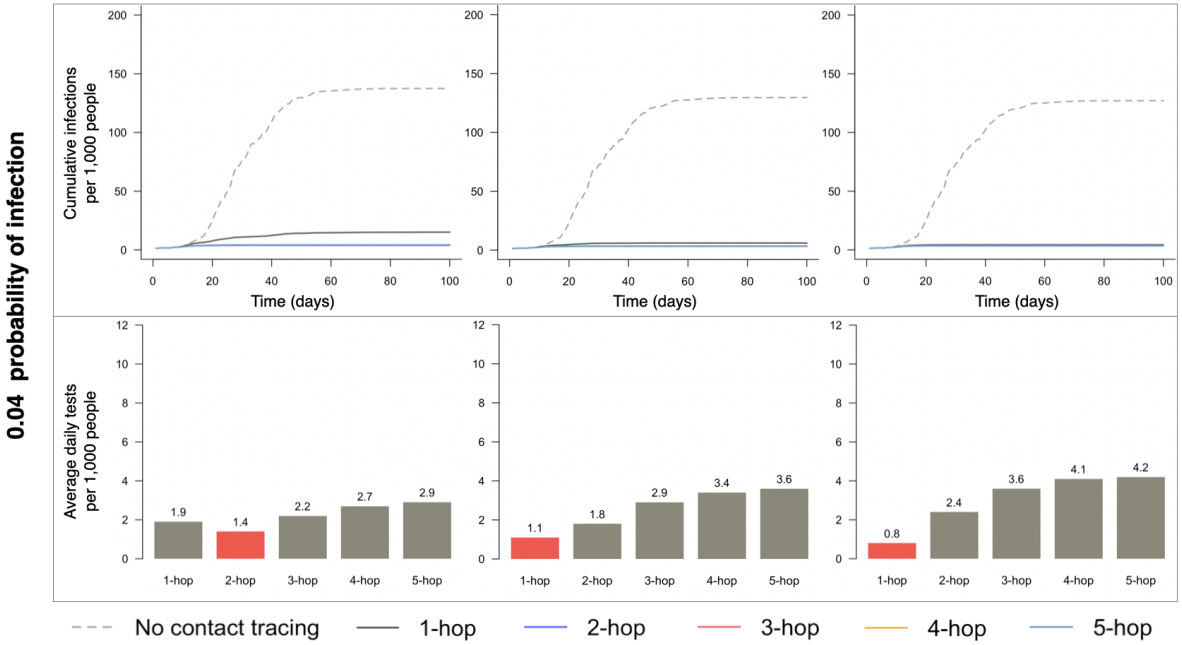

Figure 7: **The cumulative number of infections and average daily tests required for k-hop contact tracing for various values of k for data-driven time-varying network.** *The probability of infection is* 0.04*. The red colored bar corresponds to the threshold value of* k*. For* k *exceeding the threshold value, the curves for the cumulative number of infections heavily overlap and become indistinguishable.*

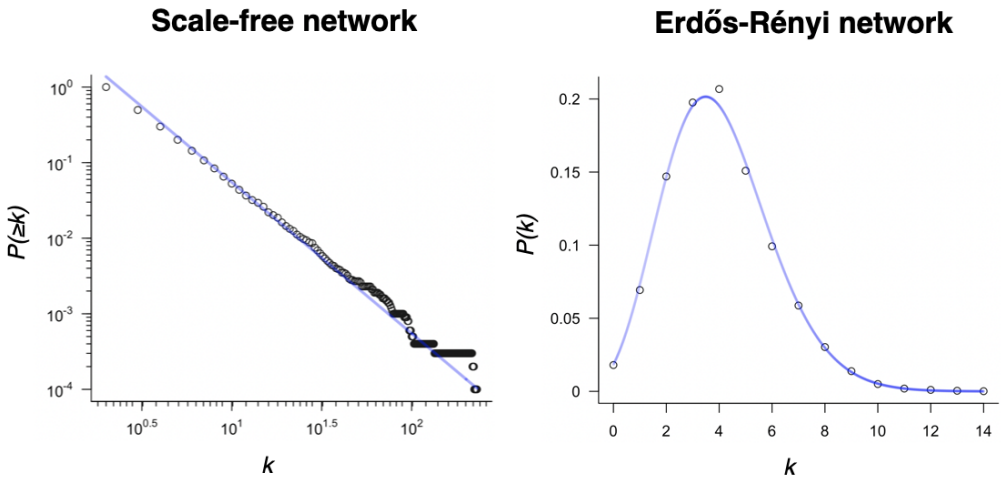

(a) (b)

Figure 8: **Degree distribution of the respective network realizations of the scale-free and Erdős Rényi network used for the data plotted in Figures 5 and 6.** *(a) The points represent the cumulative degree distribution for the scale-free network, and the slope of the line is* 2 *which is the theoretical exponent of this power-law distribution. Those are plotted on a double logarithmic scale. (b) The points represent the degree distribution for the Erdős Rényi network, and the line represents the Poisson distribution with parameter* 4.

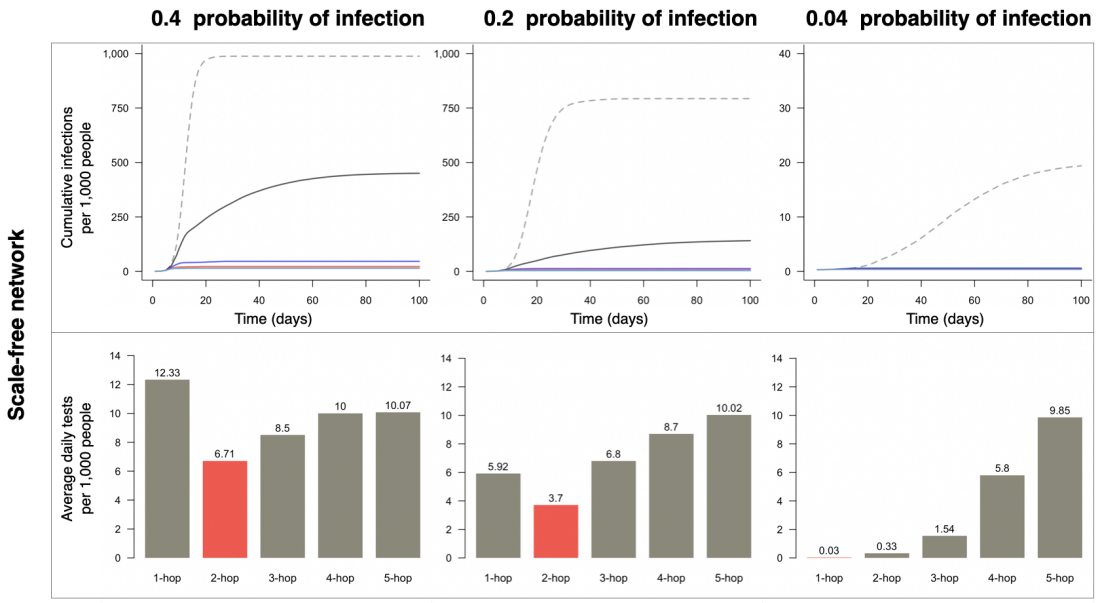

(a)

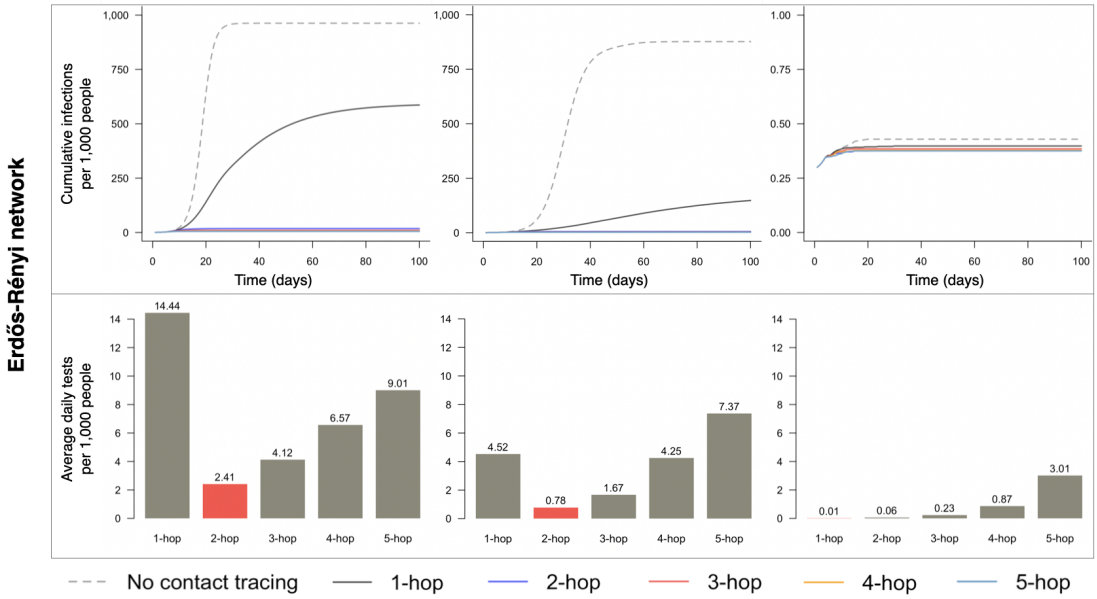

(b)

Figure 9: **Cumulative infection count and total number of tests needed for multi-hop contact tracing policy.** *The data has been obtained for the same setups as in Figure 5, only difference is that this figure plots the results averaged over* 10 *network realizations and* 100 *simulation runs on each network realization, while Figure 5 plots the results averaged over* 1000 *simulation runs over* 1 *network realization. This figure closely resembles Figure 5 both in overall trends and specific values of the data points.*

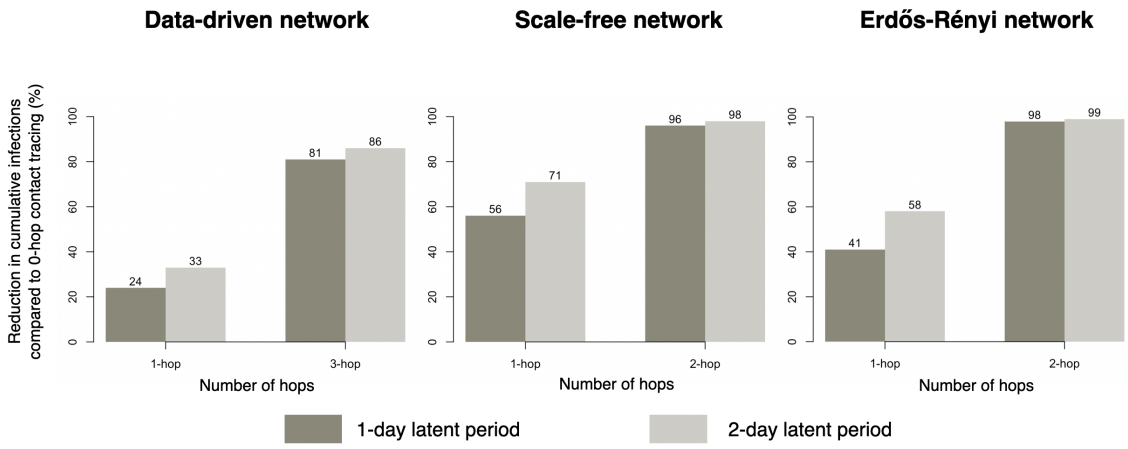

Figure 10: **Comparison of cumulative infection for different values of mean latency period.** *We use probability of infection as* 0.4*. The cooperativities are* 0.2 *and* 1 *respectively for data-driven time-varying network and static synthetic networks. The plots compare the numbers for* 1*-hop and* k*-hop contact tracings when* k *equals the corresponding threshold value.*

Table 1: Values of disease parameters

Parameter	**Notation**	**Value**	**Reference & Description**
Probability of infection (Probability with which a symptomatic individual infects a susceptible in an interaction)	β_s	0.4, 0.2, 0.04	Assumed various scenarios
Infectiousness of presymptomatic individuals relative to symptomatic	γ_p	1	Inferred from [10] suggesting significant presymptomatic transmission
Infectiousness of asymptomatic individuals relative to symptomatic	γ_a	0.75	Best estimate by [21] from prior studies [13],[27],[26],[15],[17]
Proportion of infections that are asymptomatic	p_a	0.4	[21],[18]
Mean latency period †	$1/\lambda$	1, 2 days	Inferred from [16]
Mean duration in asymptomatic stage	$1/r_a$	7 days	Inferred from [5],[16]
Mean incubation period (period between infection and the onset of symptoms)	$1/\lambda + 1/\alpha$	5 days	[14],[12]
Mean duration from symptom onset to testing	$1/w$	4 days	Inferred from [4]
Mean duration of symptom onset to recovery or death	$1/w + 1/r_s$	14 days	Inferred from [20], [5]
Fraction of symptomatics who die	p_d	0.0065	[21]

† All Figures use a mean latency period of 1, except Figure 10 in which we compare the results for mean latency periods of 1 and 2.